Time-harmonic response of a horizontal electric dipole in a layered earth with arbitrary anisotropy

Changchun Yin (Braunschweig) and Hans-Martin Maurer (Houston)

1 Abstract

The traditional model for the interpretation of geoelectromagnetic data is a layered isotropic earth, but in regions with distinct dipping stratification this model is inadequate. Furthermore, because of the great memory and time requirements it is as well impossible to simulate these structures with a 3D-model. In this case it is useful to extend this layered isotropic model to a layered earth with general anisotropy, such that to each layer is assigned a symmetrical (3×3) - resistivity tensor.

Two scalar potentials are introduced to solve the Maxwell's equations for the electromagnetic (EM) fields, which describe the poloidal and toroidal part of the magnetic field, respectively. Through a 2D-Fourier-transform, Maxwell's equations in space domain are converted into two coupled differential equations for the potentials in the wavenumber domain. In order to stabilize the numerical calculation, the wavenumber domain is divided into two parts. Whereas the EM fields with small wavenumbers are calculated by the continuation with the conditions of continuity from layer to layer, a Green's function is applied for the calculation of EM fields with great wavenumbers.

CSAMT apparent resistivies and the EM fields in the earth are calculated for the model of a layered earth with arbitrary anisotropy. In comparison with the case of an isotropic earth, both the EM fields and the apparent resistivities are disturbed in a complicated way by the anisotropy of the earth.

2 Introduction

Magnetotellurics (MT) is a geophysical prospecting method, where the magnetic fields and the horizontal electrical fields are recorded. From the frequency and the space dependence of these fields it is possible to draw conclusions on the electrical conductivity distribution in the earth. While the passive MT method uses the natural EM field, the Controlled Source Audio-magnetotellurics (CSAMT) method uses as source a grounded horizontal electric dipole or a horizontal loop as vertical magnetic dipole. In this way it is possible to have good results even in the region with large cultural noise.

The effect of the anisotropy of the earth on the geoelectromagnetic measurements has been realized at the beginning of sixties, but much attention has been payed only to the effect on the passive MT method. The problem of finding the EM fields for an anisotropic earth induced by plane-wave was solved by Mann (1965), O'Brien and Morrison (1967), Reddy and Rankin (1971), Loewenthal and Landisman (1973), Abramovici (1974), Shoham and Loewenthal (1975), Dekker and Hastie (1980), Morgan, Fisher and Milne (1987). The EM induction by an artificial source for a transverse isotropic earth is dealt with by Sinha and Bhattacharya (1967), Chlamtac and Abramovici (1981) *et al.* Li and Pedersen (1991,1992) calculated the EM response for a azimuthal anisotropic earth. Combee (1991) calculated the EM fields of an electric dipole for an anisotropic earth in the time domain. Maurer (1993) treated with the EM induction in an arbitrary anisotropic half-space. Yin and Weidelt (1998) have developed an algorithm to calculate the electric and magnetic fields in direct current prospecting for a layered earth with arbitrary anisotropy, which builds also part of the algorithm of this paper.

In this paper we have treated the general problem of the EM induction in a layered earth with arbitrary anisotropy, where the source is electric dipole. CSAMT apparent resistivities and the EM fields in the earth have been calculated.

3 Basic equations

In geoelectromagnetic prospecting the EM fields **E**, **H**, **B** and the current density **J** satisfy the following Maxwell's equations:

$$\nabla \times \mathbf{E} = -i\omega \mathbf{B}, \qquad \nabla \cdot \mathbf{J} = 0, \tag{1}$$
$$\nabla \times \mathbf{H} = \mathbf{J}, \qquad \nabla \cdot \mathbf{B} = 0, \tag{2}$$

where the harmonic time dependence $e^{i\omega t}$ and the quastatic approximation are assumed and $\mathbf{J} = \underline{\underline{\sigma}}\,\mathbf{E} + \mathbf{J_e}$. Here $\mathbf{J_e}$ is the source current density and

$$\underline{\underline{\sigma}} = \underline{\underline{\rho}}^{-1}, \quad \underline{\underline{\rho}} = \begin{pmatrix} \rho_{xx} & \rho_{xy} & \rho_{xz} \\ \rho_{xy} & \rho_{yy} & \rho_{yz} \\ \rho_{xz} & \rho_{yz} & \rho_{zz} \end{pmatrix} \tag{3}$$

are conductivity and resistivity tensor, respectively. In the earth these tensors are symmetric and positive-definite. The latter is required to ensure that the specific energy dissipation $\mathbf{E}\,\underline{\underline{\sigma}}\,\mathbf{E}$ is positive. In the air we assume $\underline{\underline{\sigma}} = \underline{\underline{0}}$. The magnetic permeability of the earth is assumed to be constant everywhere and equal to the vacuum permeability μ_0.

Equations (1) and (2) show that the magnetic field $\mathbf{H} = \mathbf{B}/\mu_0$ and the current density **J** are solenoidal vector fields. Therefore we can represent each of these fields by a toroidal and a poloidal scalar, *i.e.*

$$\mathbf{H} = \nabla \times (\hat{\mathbf{z}} T_H) + \nabla \times \nabla \times (\hat{\mathbf{z}} P_H), \tag{4}$$
$$\mathbf{J} = \nabla \times (\hat{\mathbf{z}} T_J) + \nabla \times \nabla \times (\hat{\mathbf{z}} P_J), \tag{5}$$

where $\hat{\mathbf{z}}$ is a unit vector in vertical direction of the Cartesian coordinate system with the air-earth interface as origin of the z-coordinate.

In the horizontal wavenumber domain with $k := |\mathbf{k}|$, $\mathbf{k} = u\hat{\mathbf{x}} + v\hat{\mathbf{y}} = k(\cos\beta\hat{\mathbf{x}} + \sin\beta\hat{\mathbf{y}})$, all fields are identified by a tilde and are connected with the corresponding fields in the space domain by

$$F(x,y) = \frac{1}{4\pi^2} \iint\limits_{-\infty}^{+\infty} \tilde{F}(u,v) e^{i(ux+vy)} du dv. \tag{6}$$

Equations (4) and (5) yield as representation of the Cartesian components of $\tilde{\mathbf{J}}$ and $\tilde{\mathbf{H}}$

$$\tilde{\mathbf{J}} = \begin{pmatrix} iv\tilde{T}_J + iu\tilde{P}'_J \\ -iu\tilde{T}_J + iv\tilde{P}'_J \\ k^2\tilde{P}_J \end{pmatrix}, \qquad \tilde{\mathbf{H}} = \begin{pmatrix} iv\tilde{T}_H + iu\tilde{P}'_H \\ -iu\tilde{T}_H + iv\tilde{P}'_H \\ k^2\tilde{P}_H \end{pmatrix}, \tag{7}$$

where the prime denotes differentiation with respect to z. From $\hat{\mathbf{z}} \cdot (\nabla \times \mathbf{H} - \mathbf{J}) = 0$ and $\hat{\mathbf{z}} \cdot \nabla \times (\nabla \times \mathbf{H} - \mathbf{J}) = 0$ follow

$$\tilde{T}_H = \tilde{P}_J, \qquad \tilde{T}_J = k^2 \tilde{P}_H - \tilde{P}_H''. \tag{8}$$

Furthermore $\hat{\mathbf{z}} \cdot \nabla \times \mathbf{E} = \hat{\mathbf{z}} \cdot \nabla \times (\underline{\underline{\rho}}\, \mathbf{J}) = 0$ and $\hat{\mathbf{z}} \cdot \nabla \times \nabla \times \mathbf{E} = \hat{\mathbf{z}} \cdot \nabla \times \nabla \times (\underline{\underline{\rho}}\, \mathbf{J}) = 0$ yield on account of equation (8) within uniform layers

$$a\tilde{P}_H'' - (k^2 a + i\omega\mu_0)\tilde{P}_H - b\tilde{P}_J' + ic\tilde{P}_J = 0, \tag{9}$$
$$d\tilde{P}_J'' + 2e\tilde{P}_J' + (c^2 - af)\tilde{P}_J - i\omega\mu_0 b\tilde{P}_H' - \omega\mu_0 c\tilde{P}_H = 0, \tag{10}$$

where

$$a := \rho_{xx}\sin^2\beta - 2\rho_{xy}\sin\beta\cos\beta + \rho_{yy}\cos^2\beta, \tag{11}$$
$$b := \rho_{xy}(\sin^2\beta - \cos^2\beta) + (\rho_{xx} - \rho_{yy})\sin\beta\cos\beta, \tag{12}$$
$$c := k(\rho_{xz}\sin\beta - \rho_{yz}\cos\beta), \tag{13}$$
$$d := \rho_{xx}\rho_{yy} - \rho_{xy}^2, \tag{14}$$
$$e := ik[(\rho_{xz}\rho_{xy} - \rho_{yz}\rho_{xx})\sin\beta + (\rho_{yz}\rho_{xy} - \rho_{xz}\rho_{yy})\cos\beta], \tag{15}$$
$$f := i\omega\mu_0 + \rho_{zz}k^2. \tag{16}$$

At internal layer boundaries, the vector $\mathbf{H}$, the normal component of $\mathbf{J}$, and the tangential component of $\mathbf{E}$ are continuous. This implies

$$[\tilde{P}_H] = 0, \quad [\tilde{P}_H'] = 0, \quad [\tilde{P}_J] = 0, \quad [(-i\omega\mu_0 b\tilde{P}_H + d\tilde{P}_J' + e\tilde{P}_J)/a] = 0. \tag{17}$$

where [ ] means the jump of the function across the boundary.

The current sources, assumed at $z = 0$, are incorporated by the jump conditions (Yin and Weidelt, 1998)

$$-[\tilde{P}_H']_-^+ = \tilde{P}_H'(0^-) - \tilde{P}_H'(0^+) = k\tilde{P}_H(0) - \tilde{P}_H'(0^+) =: D_H, \tag{18}$$

$$[\tilde{P}_J]_-^+ = \tilde{P}_J(0^+) =: D_J, \tag{19}$$

where $[\varphi]_-^+ := \varphi(0^+) - \varphi(0^-)$. In order to simplify the matrix representation of the coupling to the sources later, we have introduced here in the left side of the equation (18) a minus sign. Assuming that there are two point sources feeding the current $+I$ at $\mathbf{r}_A = (x_A, y_A, 0)$ and $-I$ at $\mathbf{r}_B = (x_B, y_B, 0)$, we obtain with $\mathbf{r}_A - \mathbf{r}_B =: \hat{\mathbf{d}}\,|\mathbf{r}_A - \mathbf{r}_B|$

$$D_H = \begin{cases} -\frac{I}{k^2}\dfrac{\mathbf{k}\cdot(\hat{\mathbf{d}}\times\hat{\mathbf{z}})}{\mathbf{k}\cdot\hat{\mathbf{d}}}\{\mathrm{e}^{-i\mathbf{k}\cdot\mathbf{r}_A} - \mathrm{e}^{-i\mathbf{k}\cdot\mathbf{r}_B}\}, & \mathbf{k}\cdot\hat{\mathbf{d}} \neq 0, \\ +\frac{I}{k^2}|\mathbf{r}_A - \mathbf{r}_B| i\mathbf{k}\cdot(\hat{\mathbf{d}}\times\hat{\mathbf{z}})\mathrm{e}^{-i\mathbf{k}\cdot(\mathbf{r}_A+\mathbf{r}_B)/2}, & \mathbf{k}\cdot\hat{\mathbf{d}} = 0, \end{cases} \tag{20}$$

$$D_J = \frac{I}{k^2}\{\mathrm{e}^{-i\mathbf{k}\cdot\mathbf{r}_A} - \mathrm{e}^{-i\mathbf{k}\cdot\mathbf{r}_B}\}, \tag{21}$$

from which follow for a horizontal electric dipole with the moment $\mathbf{d} = I|\mathbf{r}_A - \mathbf{r}_B|\,\hat{\mathbf{d}} = Il\hat{\mathbf{d}}$,

$$D_H = -\frac{i(\mathbf{k}\times\hat{\mathbf{z}})\cdot\mathbf{d}}{k^2}, \quad D_J = -\frac{i\mathbf{k}\cdot\mathbf{d}}{k^2}. \tag{22}$$

4 Continuation of potentials

Figure 1 shows the model composed of L uniform anisotropic layers with the resistivity tensors $\underline{\underline{\rho}}_1 \cdots \underline{\underline{\rho}}_l \cdots \underline{\underline{\rho}}_L$, the layer thickness $h_1 \cdots h_{L-1}$ and the top layer boundaries $z_1 \cdots z_L$. In

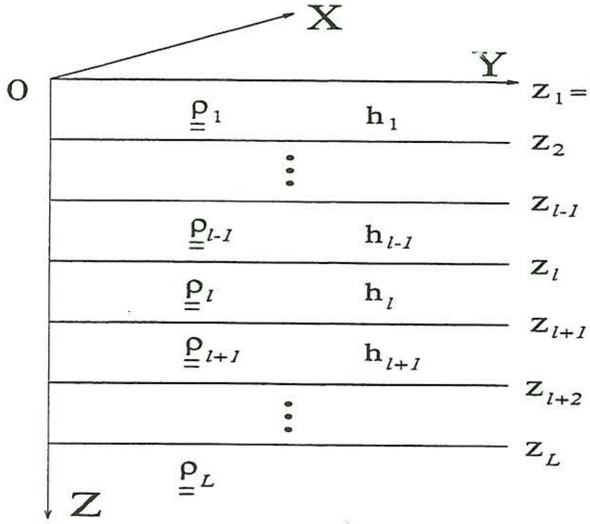

Figure 1: Layered earth with arbitrary anisotropy

each layer the solutions of (9) and (10) are of exponential type, $\tilde{P}_H \sim A_H e^{-\alpha z}$, $\tilde{P}_J \sim A_J e^{-\alpha z}$, where A_H, A_J are the amplitudes of potentials. Inserting $\tilde{P}_H$ and $\tilde{P}_J$ in equations (9) and (10) yields

$$\begin{pmatrix} \alpha^2 a - k^2 a - i\omega\mu_0 & \alpha b + ic \\ \alpha i\omega\mu_0 b - \omega\mu_0 c & \alpha^2 d - 2\alpha e + c^2 - af \end{pmatrix} \begin{pmatrix} A_H \\ A_J \end{pmatrix} = \begin{pmatrix} 0 \\ 0 \end{pmatrix}. \tag{23}$$

This system of equations is solvable, *i.e.* there exists a solution with $A_H, A_J \neq 0$, only if the determinant vanishes, which means

$$\begin{aligned} &ad\alpha^4 - 2ae\alpha^3 - (k^2 ad + i\omega\mu_0 d - ac^2 + a^2 f + i\omega\mu_0 b^2)\alpha^2 \\ &+(2k^2 ae + 2i\omega\mu_0 e + 2\omega\mu_0 bc)\alpha - k^2 ac^2 + k^2 a^2 f + i\omega\mu_0 af = 0. \end{aligned} \tag{24}$$

Equation (24) can be solved analytically with the method of the cubic resolvent (Bronstein & Semendjajew, 1979). From (23) we can also introduce the amplitude ratio:

$$\gamma_m := \frac{A_{J_m}}{A_{H_m}} = -\frac{\alpha_m^2 a - k^2 a - i\omega\mu_0}{\alpha_m b + ic} = \frac{-\alpha_m i\omega\mu_0 b + \omega\mu_0 c}{\alpha_m^2 d - 2\alpha_m e + c^2 - af}, \quad m = 1, 2, 3, 4. \tag{25}$$

Apart from the underlying half-space, the decay constants can have both signs in such a uniform layer. Therefore all four solutions of equation (24) are possible, and the potentials inside the layer l with $z_l < z < z_{l+1}$ have the form:

$$\tilde{P}_{Hl} = A_{1,l}^- e^{-\alpha_{1,l}(z-z_l)} + A_{2,l}^- e^{-\alpha_{2,l}(z-z_l)} + A_{3,l}^- e^{-\alpha_{3,l}(z-z_l)} + A_{4,l}^- e^{-\alpha_{4,l}(z-z_l)}, \tag{26}$$

$$\tilde{P}_{Jl} = \gamma_{1,l} A_{1,l}^- e^{-\alpha_{1,l}(z-z_l)} + \gamma_{2,l} A_{2,l}^- e^{-\alpha_{2,l}(z-z_l)} + \gamma_{3,l} A_{3,l}^- e^{-\alpha_{3,l}(z-z_l)} + \gamma_{4,l} A_{4,l}^- e^{-\alpha_{4,l}(z-z_l)}. \tag{27}$$

Insertion into the continuity equation (17) yields:

$$\underline{A}_l^+ = \underline{\underline{E}}_l\, \underline{A}_l^-, \quad \underline{\underline{S}}_l\, \underline{A}_l^+ = \underline{\underline{S}}_{l+1}\, \underline{A}_{l+1}^-, \tag{28}$$

where the vectors $\underline{A}_l^- := (A_{1,l}^-, A_{2,l}^-, A_{3,l}^-, A_{4,l}^-)^T$, $\underline{A}_l^+ := (A_{1,l}^+, A_{2,l}^+, A_{3,l}^+, A_{4,l}^+)^T$, while A_l^- and A_l^+ are the amplitudes of the potential at the top and bottom boundaries of layer l, respectively, and the continuity matrix $\underline{\underline{S}}_l$ and the propagation matrix $\underline{\underline{E}}_l$ are defined:

$$\underline{\underline{E}}_l : = \begin{pmatrix} e^{-\alpha_{1,l}h_l} & 0 & 0 & 0 \\ 0 & e^{-\alpha_{2,l}h_l} & 0 & 0 \\ 0 & 0 & e^{-\alpha_{3,l}h_l} & 0 \\ 0 & 0 & 0 & e^{-\alpha_{4,l}h_l} \end{pmatrix}, \tag{29}$$

$$\underline{\underline{S}}_l : = \begin{pmatrix} 1 & 1 & 1 & 1 \\ -\alpha_{1,l} & -\alpha_{2,l} & -\alpha_{3,l} & -\alpha_{4,l} \\ \gamma_{1,l} & \gamma_{2,l} & \gamma_{3,l} & \gamma_{4,l} \\ \eta_{1,l} & \eta_{2,l} & \eta_{3,l} & \eta_{4,l} \end{pmatrix}, \tag{30}$$

with $\eta_{m,l} := k^2(-i\omega\mu_0 b_l - d_l\alpha_{m,l}\gamma_{m,l} + e_l\gamma_{m,l})/a_l$.
In this way one can continue the fields from layer to layer, and connect the amplitudes of potentials on the earth surface with those at the top boundary of the underlying half-space by continuous matrix multiplication:

$$\underline{A}_L^- = (\underline{\underline{S}}_L^{-1}\underline{\underline{S}}_{L-1}\underline{\underline{E}}_{L-1}) \cdots (\underline{\underline{S}}_3^{-1}\underline{\underline{S}}_2\underline{\underline{E}}_2)(\underline{\underline{S}}_2^{-1}\underline{\underline{S}}_1\underline{\underline{E}}_1)\underline{A}_1^- = \underline{\underline{M}}\,\underline{A}_1^-. \tag{31}$$

Furthermore, in the amplitude vector at the top boundary of underlying half-space only the first two elemente are different from zero, *i.e.* $\underline{A}_L^- = (A_{1,L}^-, A_{2,L}^-, 0, 0)^T$, because the fields must vanish at great depth and thus only the exponential terms decaying with z are allowed. Two other equations follow from the coupling the sources. Inserting the equations (26) and (27) in equations (18) (19) yields

$$\underline{\underline{K}}\,\underline{A}_1^- = \begin{pmatrix} D_H \\ D_J \end{pmatrix}, \tag{32}$$

$$\underline{\underline{K}} := \begin{pmatrix} k+\alpha_{1,1} & k+\alpha_{2,1} & k+\alpha_{3,1} & k+\alpha_{4,1} \\ \gamma_{1,1} & \gamma_{2,1} & \gamma_{3,1} & \gamma_{4,1} \end{pmatrix}. \tag{33}$$

After Fuchs(1968) it is useful to divide the (4×4) matrix $\underline{\underline{M}}$ and the (2×4) matrix $\underline{\underline{K}}$ in (2×2) submatrices, because these submatrices are quadratic, this implies

$$\underline{\underline{K}} := \left(\underline{\underline{K}}_{11} \,|\, \underline{\underline{K}}_{12} \right), \qquad \underline{\underline{M}} := \left(\begin{array}{c|c} \underline{\underline{M}}_{11} & \underline{\underline{M}}_{12} \\ \hline \underline{\underline{M}}_{21} & \underline{\underline{M}}_{22} \end{array} \right), \tag{34}$$

and the equations (31) (32) then read

$$\begin{pmatrix} A_{1,L}^- \\ A_{2,L}^- \end{pmatrix} = \underline{\underline{M}}_{11} \begin{pmatrix} A_{1,1}^- \\ A_{2,1}^- \end{pmatrix} + \underline{\underline{M}}_{12} \begin{pmatrix} A_{3,1}^- \\ A_{4,1}^- \end{pmatrix}, \tag{35}$$

$$\begin{pmatrix} 0 \\ 0 \end{pmatrix} = \underline{\underline{M}}_{21} \begin{pmatrix} A_{1,1}^- \\ A_{2,1}^- \end{pmatrix} + \underline{\underline{M}}_{22} \begin{pmatrix} A_{3,1}^- \\ A_{4,1}^- \end{pmatrix}, \tag{36}$$

$$\begin{pmatrix} D_H \\ D_J \end{pmatrix} = \underline{\underline{K}}_{11} \begin{pmatrix} A_{1,1}^- \\ A_{2,1}^- \end{pmatrix} + \underline{\underline{K}}_{12} \begin{pmatrix} A_{3,1}^- \\ A_{4,1}^- \end{pmatrix}. \tag{37}$$

From (36) follow

$$\begin{pmatrix} A_{1,1}^- \\ A_{2,1}^- \end{pmatrix} = -\underline{\underline{M}}_{21}^{-1}\underline{\underline{M}}_{22}\begin{pmatrix} A_{3,1}^- \\ A_{4,1}^- \end{pmatrix}, \tag{38}$$

$$\begin{pmatrix} A_{3,1}^- \\ A_{4,1}^- \end{pmatrix} = -\underline{\underline{M}}_{22}^{-1}\underline{\underline{M}}_{21}\begin{pmatrix} A_{1,1}^- \\ A_{2,1}^- \end{pmatrix}. \tag{39}$$

(39) inserted in (37) gives

$$\begin{pmatrix} A_{1,1}^- \\ A_{2,1}^- \end{pmatrix} = (\underline{\underline{K}}_{11} - \underline{\underline{K}}_{12}\underline{\underline{M}}_{22}^{-1}\underline{\underline{M}}_{21})^{-1}\begin{pmatrix} D_H \\ D_J \end{pmatrix}, \tag{40}$$

and (38) inserted in (37) gives

$$\begin{pmatrix} A_{3,1}^- \\ A_{4,1}^- \end{pmatrix} = (\underline{\underline{K}}_{12} - \underline{\underline{K}}_{11}\underline{\underline{M}}_{21}^{-1}\underline{\underline{M}}_{22})^{-1}\begin{pmatrix} D_H \\ D_J \end{pmatrix}. \tag{41}$$

Consequently one can get the EM fields in the earth from the solution of (40) and (41). If the measuring point at depth z is located in the layer l with $z_l < z < z_{l+1}$, then from (7) follow the EM fields in the wavenumber domain:

$$\tilde{\mathbf{J}}_l(z) = -i\sum_{m=1}^{4}\begin{pmatrix} u\alpha_{m,l}\gamma_{m,l} + v(\alpha_{m,l}^2 - k^2) \\ v\alpha_{m,l}\gamma_{m,l} - u(\alpha_{m,l}^2 - k^2) \\ ik^2\gamma_{m,l} \end{pmatrix} A_{m,l}^- e^{-\alpha_{m,l}(z-z_l)}, \tag{42}$$

$$\tilde{\mathbf{H}}_l(z) = -i\sum_{m=1}^{4}\begin{pmatrix} u\alpha_{m,l} - v\gamma_{m,l} \\ v\alpha_{m,l} + u\gamma_{m,l} \\ ik^2 \end{pmatrix} A_{m,l}^- e^{-\alpha_{m,l}(z-z_l)}. \tag{43}$$

In principle it is possible to calculate the EM fileds in a layered earth with arbitrary anisotropy in this way. The implementation leads, however, to numerical problems. From the four solutions of equation (24) two of which have always a positive and two of which a negative real part, which imply downgoing and upgoing waves, respectively, thus the propagation matrix $\underline{\underline{E}}$ contains the exponential terms with both signs. For great wavenumbers or great layer thickness the representable number range of computer is quickly exceeded and this leads to numerical instability. Therefore by numerical handling we divide the wavenumber domain into two parts. The continuation method which we have described is used only to calculate the EM fields with small wavenumbers. The method calculating the EM fields with great wavenumbers is dealt with by Yin and Weidelt (1998).

5 Numerical results

5.1 Impedance tensor and CSAMT apparent resistivity

Theoretically one can prove that in CSAMT the impedance tensor is independent of the orientation of the dipole sources (Li and Pedersen,1991), therefore one can calculate the impedance tensor elements from the fields of two electric dipoles with subscripts 1,2 oriented in x- and y direction:

$$E_{x1} = Z_{xx}H_{x1} + Z_{xy}H_{y1}, \quad E_{y1} = Z_{yx}H_{x1} + Z_{yy}H_{y1}, \tag{44}$$
$$E_{x2} = Z_{xx}H_{x2} + Z_{xy}H_{y2}, \quad E_{y2} = Z_{yx}H_{x2} + Z_{yy}H_{y2}. \tag{45}$$

From (44) (45) we get the tensor elements:

$$Z_{xx} = (E_{x1}H_{y2} - E_{x2}H_{y1})/\zeta, \quad Z_{xy} = (E_{x2}H_{x1} - E_{x1}H_{x2})/\zeta, \tag{46}$$
$$Z_{yx} = (E_{y1}H_{y2} - E_{y2}H_{y1})/\zeta, \quad Z_{yy} = (E_{y2}H_{x1} - E_{y1}H_{x2})/\zeta, \tag{47}$$
$$\text{with} \quad \zeta = H_{y2}H_{x1} - H_{y1}H_{x2}, \tag{48}$$

the apparent resistivities and the phases:

$$\rho_{xy} = \frac{1}{\omega\mu_0} \mid Z_{xy} \mid^2, \quad \phi_{xy} = tan^{-1}[Im(Z_{xy})/Re(Z_{xy})], \tag{49}$$
$$\rho_{yx} = \frac{1}{\omega\mu_0} \mid Z_{yx} \mid^2, \quad \phi_{yx} = tan^{-1}[Im(Z_{yx})/Re(Z_{yx})]. \tag{50}$$

Fig. 2 shows the comparison between the numerical results of this paper and those of Li and Pedersen(1992) for a two-layer model with an isotropic top layer over an azimuthal anisotropic half-space. The results, presented as the effective apparent resistivity and the effective phase, as defined by Li and Pedersen, show excellent agreement.

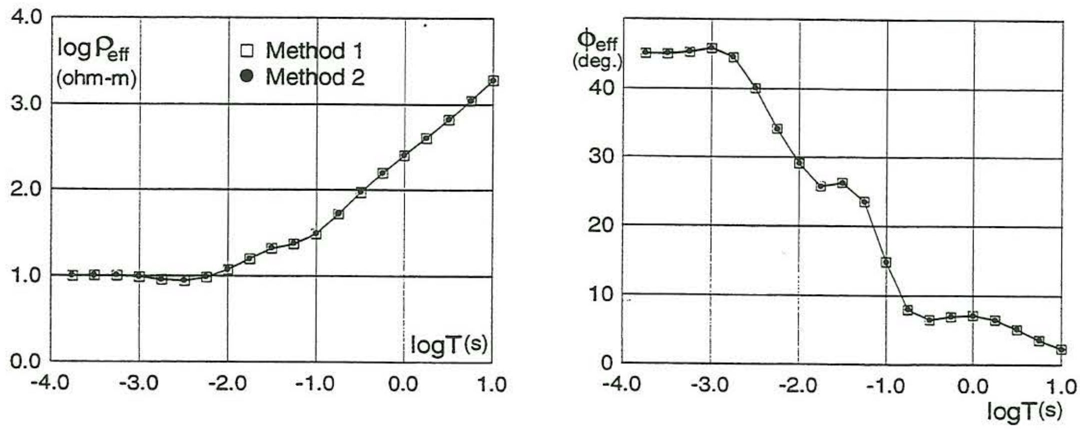

Figure 2: Comparison of the calculation results of this paper (Method 1) with those from Li and Pedersen (Method 2) for a two-layer model with an isotropic top layer ($\rho_1 = 10\ \Omega$m, $h_1 = 100$ m) over an azimuthal anisotropic half-space ($\rho_{xx} = \rho_{zz} = 50\ \Omega$m, $\rho_{yy} = 200\ \Omega$m, $\rho_{xy} = \rho_{xz} = \rho_{yz} = 0$), the measuring point is located in $x = y = 3000$ m. The definition of ρ_{eff} and ϕ_{eff} is that of Li and Pedersen (1992).

Fig. 3 shows the CSAMT apparent resistivities and the phases defined in this paper for a two-layer model. The overburden is isotropic and conductive. But the substratum is anisotropic and its resistivity tensor changes.

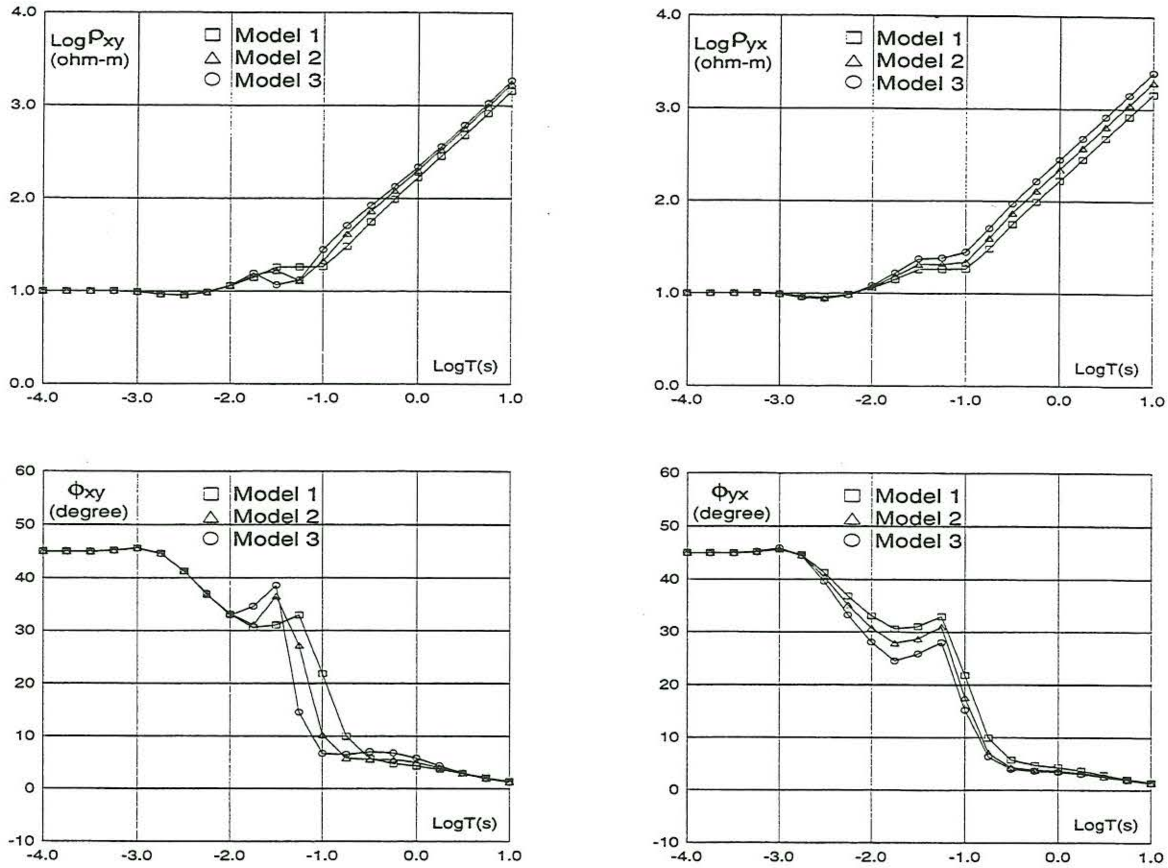

Figure 3: CSAMT apparent resistivities and phases. Three models have the same conductive overburden ($\rho_1 = 10\ \Omega$m, $h_1 = 100$ m), but different dipping anisotropic substrata. These three anisotropic substrata can be obtained through the rotation of 3 azimuthal anisotropic half-spaces ($\rho_{xx} = \rho_{zz} = 50\ \Omega$m, ρ_{yy} changes – Model 1: 50 Ωm, Model 2: 100 Ωm, Model 3: 200 Ωm) anticlockwise by 45^0 around the x-axis, $x = y = 3000$ m.

These figures indicate that

a) by high frequency the apparent resistivies and the phases are not influenced by the anisotropy of the substratum, the apparent resistivities and the phases depend mainly on the resistivity of the isotropic top layer;

b) with the decrease of the frequency the influence of the anisotropy of the substratum becomes more and more distinct;

c) the anisotropy of the earth is resolvable particularly from the phases.

5.2 Distribution of the EM fields in the earth

The current densities in the earth are calculated for a two-layer model and shown as arrows in Figure 4. The top layer is isotropic ($\rho_1 = 100\ \Omega$m, $h_1 = 1300$ m) and the underlying half-space is dipping anisotropic, which can be obtained through the rotation of an azimuthal anisotropic half-space ($\rho_{xx} = \rho_{zz} = 50\ \Omega$m, $\rho_{yy} = 400\ \Omega$m) anticlockwise by 45^0 around the x-axis. The fields are multiplied by r^3 at each point, which is equivalent to the normalization by the far-field, where r is the distance between measuring points and electric dipole. The electric dipole is located in y-direction and shown in the figures, the frequency of the field is $f = 10$ Hz.

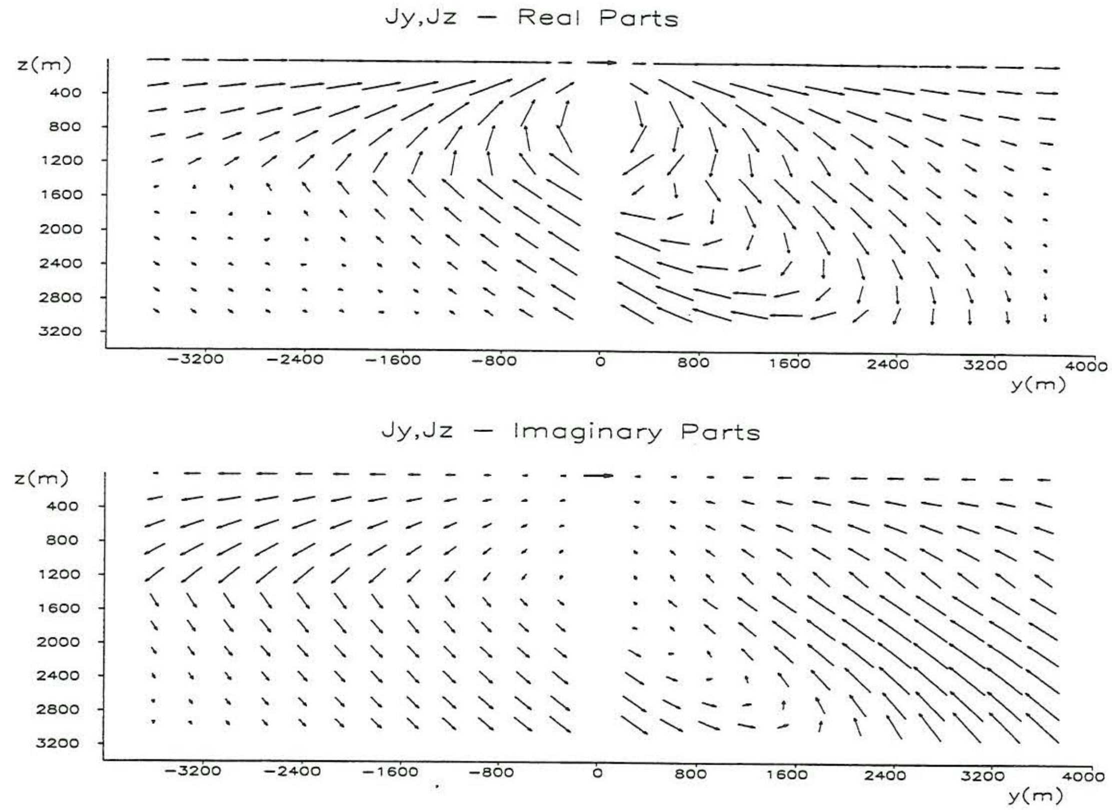

Figure 4: Distribution of the real and imaginary part of the current density in the earth. The electric dipole is in y-direction.

From both figures we conclude that

a) In the underlying half-space the current flows mainly in the dipping direction of stratification, where the current channelling exists;

b) The boundary surface and the anisotropy of the earth can be clearly distinguished.

6 Conclusions

Using the field representation of the current density and the magnetic field in terms of poloidal and toroidal scalars, we have developed an algorithm to calculate the EM induction for a layered earth with arbitrary anisotropy. In the wavenumber domain different methods are used to calculate the EM fields according to the wavenumber. The field-components with small wavenumbers we have continued from layer to layer with the continuity conditions. The field-components with great wavenumbers have to be calculated with the method developed by Yin and Weidelt (1998). As the first application of the algorithm of this paper we have calculated CSAMT apparent resistivities and phases and presented the EM fields inside the earth. The calculation results for different models show that the anisotropy of the earth can be solved from both the apparent resistivities and the phases on the earth surface. The distributions of EM fields in the earth reflect as well the boundary surface and the electric character of earth.

7 References

Abramovici, F., 1974, The forward magnetotelluric problem for an inhomogeneous and anisotropic structure: Geophysics, **39**, 56-68.

Bronstein, I.N., and Semendjajew, K.A., 1979, Taschenbuch der Mathematik: B.G. Teubner Verlagsgesellschaft, Leipzig.

Chlamtac, M., and Abramovici, F., 1981, The electromagnetic fields of a horizontal dipole over a vertically inhomogeneous and anisotropic earth: Geophysics, **46**, 904-915.

Combee, L., 1991, Transient diffusive electromagnetic fields in layered anisotropic media: Delft University Press, Delft.

Dekker, D.L., and Hastie, L.M., 1980, Magneto-telluric impedances of an anisotropic layered earth model: Geophys. J. R. astr. Soc., **61**, 11-20.

Fuchs, K., 1968, Das Reflexions- und Transmissionsvermoegen eines geschichteten Mediums mit beliebiger Tiefenverteilung der elastischen Moduln und der Dichte fuer schraegen Einfall ebener Wellen: Zeitschrift fuer Geophysik, **34**, 389-413.

Li, X., and Pedersen, L.B., 1991, The electromagnetic response of an azimuthally anisotropic half-space: Geophysics, **56**, 1462-1473.

Li, X., and Pedersen, L.B., 1992, Controlled - source tensor magnetotelluric responses of a layered earth with azimuthal anisotropy: Geophys. J. Int., **111**, 91-103.

Loewenthal, D., and Landisman, M., 1973, Theory for magnetotelluric observation on the surface of a layered anisotropic half-space: Geophys. J. R. astr. Soc., **35**, 195-214.

Mann, J.E., 1965, The importance of anisotropic conductivity in magnetotelluric interpretation: J. Geophys. Res., **70**, 2940-2942.

Maurer, H.-M., 1993, Electromagnetische Induktion in anisotropen Leitern: Ph.D. Thesis, Technical University of Braunschweig, FRG.

Morgan, M.A., Fisher, D.L. and Milne, E.A., 1987, Electromagnetic scattering by stratified inhomogeneous anisotropic media: IEEE Trans. Antennas Propagat., **35**, 191-197.

O'Brien, D.P., and Morrison, H.F., 1967, Electromagnetic fields in an n-layer anisotropic half-space: Geophysics, **32**, 668-677.

Reddy, I.K. and Rankin, D., 1971, Magnetotelluric effect of dipping anisotropies: Geophys. Prosp., **19**, 84-97.

Shoham, Y., and Loewenthal, D. 1975, Matrix polynomial representation of the anisotropic magnetotelluric impedance tensor: Phys. Earth Planet. Int., **11**, 128-138.

Sinha, A.K., and Bhattacharya, P.K., 1967, Electric dipole over an anisotropic and inhomogeneous earth: Geophysics, **32**, 652-667.

Yin, Ch., and Weidelt, P., 1998, Geoelectrical fields in a layered earth with arbitrary anisotropy: Geophysics, to be published.